Quantifying Uncertainties in Land-Surface Microwave Emissivity Retrievals

Yudong Tian, Christa D. Peters-Lidard, Kenneth W. Harrison, Catherine Prigent, Hamidreza Norouzi, Filipe Aires, Sid-Ahmed Boukabara, Fumie A. Furuzawa, and Hirohiko Masunaga

***Abstract*— Uncertainties in the retrievals of microwave land-surface emissivities are quantified over two types of land surfaces: desert and tropical rainforest. Retrievals from satellite-based microwave imagers, including the Special Sensor Microwave Imager, the Tropical Rainfall Measuring Mission Microwave Imager, and the Advanced Microwave Scanning Radiometer for Earth Observing System, are studied. Our results show that there are considerable differences between the retrievals from different sensors and from different groups over these two land-surface types. In addition, the mean emissivity values show different spectral behavior across the frequencies. With the true emissivity assumed largely constant over both of the two sites throughout the study period, the differences are largely attributed to the systematic and random errors in the retrievals. Generally, these retrievals tend to agree better at lower frequencies than at higher ones, with systematic differences ranging 1%–4% (3–12 K) over desert and 1%–7% (3–20 K) over rainforest. The random errors within each retrieval dataset are in the range of 0.5%–2% (2–6 K). In particular, at 85.5/89.0 GHz, there are very large differences between the different retrieval datasets, and within each retrieval dataset itself. Further investigation reveals that these differences are most likely caused by rain/cloud contamination, which can lead to random errors up to 10–17 K under the most severe conditions.**

***Index Terms*— Brightness temperature, land-surface emissivity, measurement uncertainty, microwave radiometry, random errors, remote sensing, systematic errors.**

Manuscript received April 20, 2012; revised October 24, 2012; accepted January 23, 2013. Date of publication March 21, 2013; date of current version December 12, 2013. This work was supported by the National Aeronautics and Space Administration Precipitation Science Program under Solicitation NNH09ZDA001N.

Y. Tian and K. W. Harrison are with the Earth System Science Interdisciplinary Center, University of Maryland, College Park, MD 20740 USA (e-mail: yudong.tian@nasa.gov; Kenneth.W.Harrison@nasa.gov).

C. D. Peters-Lidard is with the Goddard Space Flight Center, NASA, Greenbelt, MD 20771 USA (e-mail: christa.peters@nasa.gov).

C. Prigent is with the Laboratoire d'Etudes du Rayonnement et de la Matière en Astrophysique, Paris Observatory, Centre National de la Recherche Scientifique, Paris 75007, France (e-mail: catherine.prigent@obspm.fr).

H. Norouzi is with the New York City College of Technology, The City University of New York, New York, NY 11201 USA (e-mail: hnorouzi@citytech.cuny.edu).

F. Aires is with Estellus, New York, NY 10022 USA (e-mail: filipe.aires@estellus-usa.com).

S.-A. Boukabara is with the National Environmental Satellite Data and Information Service, NOAA, Camp Springs, MD 20746 USA (e-mail: sid.boukabara@noaa.gov).

F. A. Furuzawa and H. Masunaga are with the Hydrospheric Atmospheric Research Center, Nagoya University, Nagoya 464-8601, Japan (e-mail: akimoto@hyarc.nagoya-u.ac.jp; masunaga@hyarc.nagoya-u.ac.jp).

Color versions of one or more of the figures in this paper are available online at http://ieeexplore.ieee.org.

Digital Object Identifier 10.1109/TGRS.2013.2244214

I. Introduction

LAND surface emissivity at microwave frequencies contains a wealth of information on the physical, biological, and hydrological states and processes of the earth's surface. This forms the basis for remote sensing of a wide range of land-surface states and processes such as soil moisture, vegetation characteristics, and land-cover dynamics [1]. In addition, land-surface emissivity acts as the background signal for the retrieval of atmospheric variables, such as water vapor, rainfall, and snowfall, and therefore greatly affects the accuracy and uncertainty in such measurements [2], [3].

Satellite-based emissivity retrievals have been performed for nearly three decades [4]–[9], while the methodology remains largely unchanged. Microwave emissivities are derived from satellite-based observations though radiative transfer calculations. Microwave radiometers onboard polar-orbiting satellites produce brightness temperature (Tb) measurements at the top of the atmosphere (TOA). With atmospheric temperature and moisture profile data, one can remove the portion of Tb originated from the atmosphere, to obtain the microwave emission from the land surface. Subsequently the land-surface emissivity can be computed if the surface temperature effective for the emission is known. More recently, the retrieval of emissivity has also been implemented in a variational [10] and/or iterative [11] framework in which many variables affecting the radiative transfer processes, including emissivity, can be estimated simultaneously.

Usually, emissivity retrievals are only performed for clear days, due to the difficulty in estimating the atmospheric contribution from a cloudy or rainy atmosphere, and to the strong atmospheric scattering and absorption of land-surface signals under such conditions, especially at higher frequencies. However, even for a cloud-free atmosphere, there are many error sources that lead to uncertainties in emissivity retrievals, including instrumental errors, inaccuracies in the atmospheric profile data, imperfect cloud screening, and misrepresentation of the land-surface temperature [7], [14], [15]. In addition, the heterogeneity of the land-surface radiometric properties and the shifts in instrument footprint locations introduce sampling errors that enhance the uncertainties.

Despite its importance, the uncertainty in emissivity retrievals has not been well quantified. This is reflected in the considerable disagreements among the most recent, state-of-the-art datasets [16]. The leading difficulty is the lack of

TABLE I
FREQUENCIES OF THE MICROWAVE IMAGERS

Frequencies of Microwave Imagers (GHz)						
SSM/I			19.35	22.2 (V)	37.0	85.5
TMI		10.65	19.35	21.3 (V)	37.0	85.5
AMSR-E	6.9	10.65	18.7	23.8	36.5	89.0

"ground-truth" data, especially on the global scale. Most of the field campaigns for land emissivity studies are short-lived and small-scale ones, and generally they are not carried out in coordination with any specific satellite-based instruments or overpasses. Without reliable reference data, the immediate impediment to uncertainty quantification is the inability to apportion the variability to measurement error or to natural variability of the land-surface emissivity.

In this paper, we circumvent this difficulty by strategically selecting two types of land surfaces whose emissivities are largely constant: the Sahara Desert and the Amazon Rainforest. Then all the variations within a set of retrievals are caused by the uncertainties, defined as the spread among independent measurements. Although this paper is limited to these two types of land surfaces, it represents a practical effort to make progress in solving an otherwise intractable problem. Thus, this paper not only provides the first quantitative results, but also facilitates more educated inference on the magnitude of uncertainty over other surfaces.

The emissivity datasets and methodology we employed are described in the following section. In Section III, we provide observational evidence to substantiate our assumption of the constant emissivity over the desert and rainforest areas. Based on such an assumption, we present results in Section IV to quantify the uncertainties. The results are then summarized and discussed in Section V.

II. DATA AND METHODOLOGY

To support the upcoming Global Precipitation Measurement (GPM) mission, NASA's Precipitation Measurement Missions (PMM) Science Team formed the Land-Surface Working Group (LSWG) to improve land-surface characterization at microwave frequencies. LSWG has assembled a collection of clear-sky land-surface emissivity retrievals from many contemporary space-borne passive microwave sensors, over selected, representative land-surface types such as desert, rainforest, midlatitude agricultural land, wet land, and high-latitude cold regions [16]. The collection of sensors includes the Special Sensor Microwave Imager (SSM/I), the Tropical Rainfall Measuring Mission (TRMM) Microwave Imager (TMI), WindSat aboard the Coriolis satellite, the Advanced Microwave Sounding Unit (AMSU), and the Advanced Microwave Scanning Radiometer for Earth Observing System (AMSR-E). This data collection greatly facilitates intercomparison and evaluation of land-surface microwave retrievals, and enables us to assess the current skills and uncertainties.

In this paper, we focus our evaluation on the three conical-scan microwave imagers: SSM/I, TMI, and AMSR-E (Table I), because they have a similarly wide frequency range, and most of their channels have both vertical and horizontal linear polarizations. Instantaneous retrievals, including both ascending and descending passes, are used whenever available. Retrievals from different data providers for the same imager are all included as independent estimates, as they are mostly derived from different algorithms and/or with different ancillary data. A common one-year period—July 1, 2006 to June 30, 2007—is used for our paper.

For SSM/I, retrievals from three Defense Meteorological Satellite Program (DMSP) platforms (F13, F14, and F15) are included. The data are provided by the Centre National de la Recherche Scientifique (CNRS), France, and the retrieval procedure is described in [6] and [8]. TMI retrievals are produced by Nagoya University, Japan, with a similar method. For AMSR-E, two independent retrieval datasets are used. One is produced by NOAA's Microwave Integrated Retrieval System (MIRS) using a 1-D variational algorithm [10], and is denoted as AMSR-E (MIRS). The other is produced by NOAA's Cooperative Remote Sensing Science and Technology Center (CREST), and the retrieval procedure is documented in [17] and [18]. This dataset is denoted as AMSR-E (CREST).

Uncertainty gauges our ignorance and state of knowledge. In practice, uncertainty can be quantified as the spread or disagreement among independent measurements of the same physical quantity. If each of the measurements has no systematic biases, then such spread arises solely from the random errors. However, most often, each measurement has distinct systematic biases that contribute to the total uncertainty. Difficulty arises when there are no "ground-truth" data available: one is not able to separate systematic errors from random ones, and either type of error from the natural variability of the measured quantity. Under these conditions, uncertainty quantification is impossible.

A practical starting point to elude this difficulty is to quantify the uncertainty over areas where the physical variable—here microwave emissivity—is constant. This is the one case in which "ground-truth" data are not needed, as all the variations in the data are from the measurement errors. One may still not be able to identify the absolute amplitude of systematic errors, but their differences among independent measurements can be obtained, and these differences provide substantial insight into their reliability as an ensemble. Moreover, the random errors can be easily quantified, which more often are the dominant part of the total uncertainty.

For this paper, we selected two land-surface types, the Sahara Desert and the Amazon Rainforest. In these regions, the desert roughness and the vegetation properties of tropical forest are not expected to change significantly with time. Since roughness and vegetation are two key controlling factors for microwave emissivity at these frequencies, they can be used as a constant-reference surface. This property has been exploited for validation and calibration of passive microwave sensors and other land-surface parameter retrievals [19]–[27]. In the following section, we will substantiate this assumption with the long-term AMSR-E observations. Though the true value of the assumed constant emissivity is unknown, we can compare the independent retrieval datasets and their disagreements to infer the magnitude of the uncertainties, including both systematic and random errors. The two sites we used in this paper are designated by LSWG as "Desert"

and "Amazon2," located at (22° N, 29° E) and (2° N, 55° W), respectively.

III. Constant Emissivity Over Study Sites

To prove that the land-surface emissivities are approximately constant over the Desert and Amazon2 sites, we examined the microwave polarization difference index (MPDI) over these two locations. MPDI is essentially a normalized measure of the polarization. The MPDI is computed from the daily AMSR-E Tb data over the three-year period of July 2004 through June 2007, for all weather conditions. Tb-based MPDI is defined as [28]–[31]

$$\mathrm{MPDI}_T = \frac{Tb_v - Tb_h}{Tb_v + Tb_h}$$

where Tb_v and Tb_h are the TOA Tb of vertical and horizontal polarization, respectively, for a specific frequency and scan angle. Similarly, emissivity-based MPDI is defined as [13]

$$\mathrm{MPDI}_\varepsilon = \frac{\varepsilon_v - \varepsilon_h}{\varepsilon_v + \varepsilon_h}$$

where ε_v and ε_h are the land-surface emissivity of vertical and horizontal polarizations, respectively, for a specific frequency and scan angle.

MPDI is closely related to the land-surface states. This is because with a clear-sky atmosphere, the polarization difference originates exclusively from the land surface; the atmosphere's attenuation and emission generate no additional polarization, serving only to suppress the polarized signals down below. Thus, Tb-based MPDI, which contains both signals from the land surface and (unpolarized) signals from the atmosphere, can be shown to be a lower-bound estimate of the emissivity-based MPDI.

For a nonscattering, plane-parallel atmosphere and for a given scan angle and frequency, the TOA brightness temperatures for vertical and horizontal polarizations can be computed by the following integrated radiative transfer equations [12], [13]:

$$\begin{aligned} Tb_v &= T_a^{\uparrow} + T_a^{\downarrow}(1-\varepsilon_v)e^{-\tau} + T_s\varepsilon_v e^{-\tau} \\ &= T_a^{\uparrow} + T_a^{\downarrow}e^{-\tau} + (T_s - T_a^{\downarrow})\varepsilon_v e^{-\tau} \qquad (1) \\ Tb_h &= T_a^{\uparrow} + T_a^{\downarrow}(1-\varepsilon_h)e^{-\tau} + T_s\varepsilon_h e^{-\tau} \\ &= T_a^{\uparrow} + T_a^{\downarrow}e^{-\tau} + (T_s - T_a^{\downarrow})\varepsilon_h e^{-\tau} \qquad (2) \end{aligned}$$

where $T_a^{\uparrow}$ and $T_a^{\downarrow}$ are the upward and downward (including cosmic background) radiations through the atmosphere, T_s the land-surface temperature, and τ the atmospheric optical depth along the view path, respectively. Then from (1) and (2) one can derive

$$\begin{aligned} \mathrm{MPDI}_T &= \frac{Tb_v - Tb_h}{Tb_v + Tb_h} \\ &= \frac{(T_s - T_a^{\downarrow})e^{-\tau}(\varepsilon_v - \varepsilon_h)}{2(T_a^{\uparrow} + T_a^{\downarrow}e^{-\tau}) + (T_s - T_a^{\downarrow})e^{-\tau}(\varepsilon_v + \varepsilon_h)} \\ &= \frac{\mathrm{MPDI}_\varepsilon}{1 + \frac{2(T_a^{\uparrow} + T_a^{\downarrow}e^{-\tau})}{(T_s - T_a^{\downarrow})e^{-\tau}(\varepsilon_v + \varepsilon_h)}} \qquad (3) \end{aligned}$$

and since $\varepsilon_v + \varepsilon_h \approx 2$ for most land surfaces, the above equation can be approximately rewritten as

$$\mathrm{MPDI}_T \approx \frac{\mathrm{MPDI}_\varepsilon}{1 + \frac{T_a^{\uparrow}e^{\tau} + T_a^{\downarrow}}{T_s - T_a^{\downarrow}}}. \qquad (4)$$

As $T_s > T_a^{\downarrow}$ for the earth's clear atmosphere in the frequency range under study, we have $\mathrm{MPDI}_T \leq \mathrm{MPDI}_\varepsilon$. In other words, the Tb-based MPDI is a lower-bound estimate of the emissivity-based MPDI. The more transparent the atmosphere is (the smaller the values of $T_a^{\uparrow}$,$T_a^{\downarrow}$, and τ are), the closer the two MPDIs will become [13].

Fig. 1 shows the Tb-based MPDI for all the six AMSR-E channels, over the Desert [Fig. 1(a)], Amazon2 [Fig. 1(b)] and a third LSWG site, the southern great plains [SGP; Fig. 1(c)]. Over the three-year period, the MPDI for both Desert and Amazon2 remains fairly constant. In contrast, SGP's MPDI values exhibit strong seasonal variations across all the channels that are related to the seasonal variations in vegetation and soil moisture. Though the data contain both clear and cloudy days, the latter only serve to further reduce MPDI values and do not obscure variations during clear days. Comparing Fig. 1(a) and (b) with (c), we can verify that our assumption of constant emissivity over Desert and Amazon2 is valid.

Over desert, the MPDI values are large, and so are the differences among the channels. This is consistent with the well-known strong polarization signature over desert areas [32]. Nevertheless, over the three-year period, the values are remarkably constant, especially for lower frequencies, which are not sensitive to the atmosphere. Slight seasonal variations are present in the water vapor channel (23.8 GHz), which suggests they are mostly atmosphere-induced. The synchronized, less-pronounced fluctuations in the 89.0-GHz channel indicate their atmospheric origin as well.

Over Amazon2 [Fig. 1(b)], the MPDI values are much lower, and close to zero for all the frequencies. This is consistent with the fact that over the dense forest the microwave signals are not strongly polarized. Despite the dense canopy, the lower frequencies exhibit slightly higher MPDI values, indicating some of the emission from either exposed soil surface or water bodies. Indeed, satellite images from Google Earth (http://earth.google.com) indicate there is a river nearby well within the sensors' footprints. The higher MPDI values are also consistent with results shown in Njoku et al.[24]. Overall, one can see MPDI remains fairly constant and very small across all the channels. Thus, it is reasonable to assume the emissivity values over Amazon2 are approximately constant too.

We also examined another arbitrarily selected, distant desert site (22° N, 5° W) and Amazon site (7° S, 70° W). The temporal variation in their respective MPDI time series is similarly small (not shown), indicating the stationarity of MPDI over these two types of surfaces a robust feature. We expect that the other imagers (SSM/I and TMI) would show the same behavior, based on results from intersensor comparison studies [19]–[27].

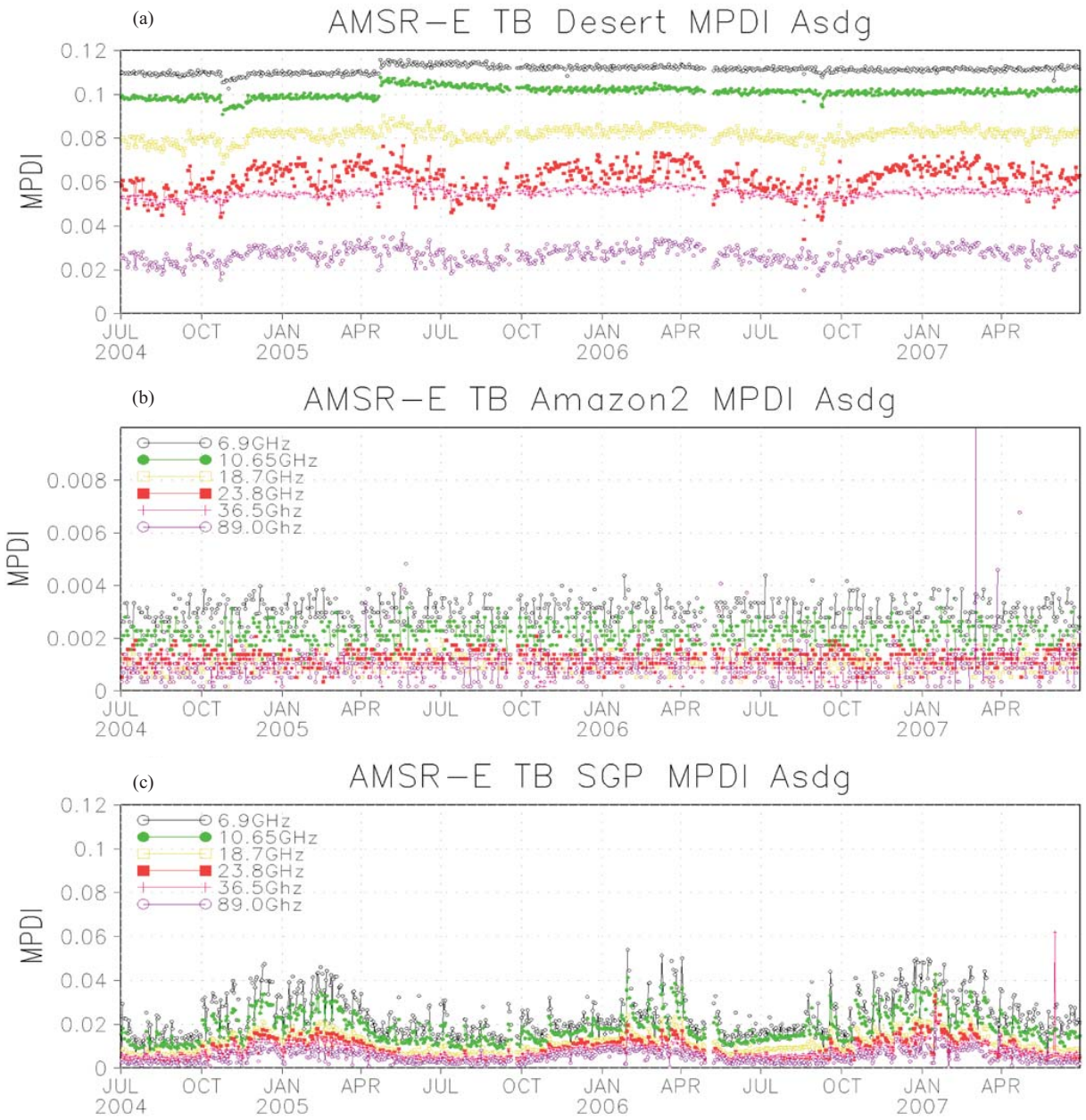

Fig. 1. MPDI calculated from AMSR-E brightness temperatures (Tb) for ascending passes over a three-year period (July 2004 through June 2007), over the three LSWG sites (a) Desert, (b) Amazon2, and (c) SGP. The cause of the discontinuities in (a) near October 2004 and April 2005 is not documented but they are confined to this particular region.

IV. Results

In this section, we first present the basic characteristics of both the systematic and random errors, including their statistical distributions shown as histograms. To gain additional insight, we then examine the errors in MPDI space, with comparisons with AMSR-E Tb data. Finally, we provide diagnostic analysis on the sources of some of the error features identified in this paper.

A. Systematic and Random Errors

Land-surface emissivity retrievals over the two evaluation sites show considerable systematic and random errors. Fig. 2 shows box-and-whisker plots for the six datasets and for both polarizations. Over the Desert site [Fig. 2(a) and (b)], the ensemble as a whole showed the expected behavior—vertically polarized emissivity decreases with frequency [Fig. 2(a)], while horizontally polarized emissivity increases [Fig. 2(b)] [32]. However, there are considerable systematic differences between the mean values from each retrieval dataset, indicating most of them, if not all, have systematic errors, regardless of the unknown "ground truth." The systematic differences are the smallest at lower frequencies (6.9 and 10.65 GHz), reflecting partly their insensitivity to atmospheric effects. The random errors also show a strong dependency on frequency. The higher frequencies

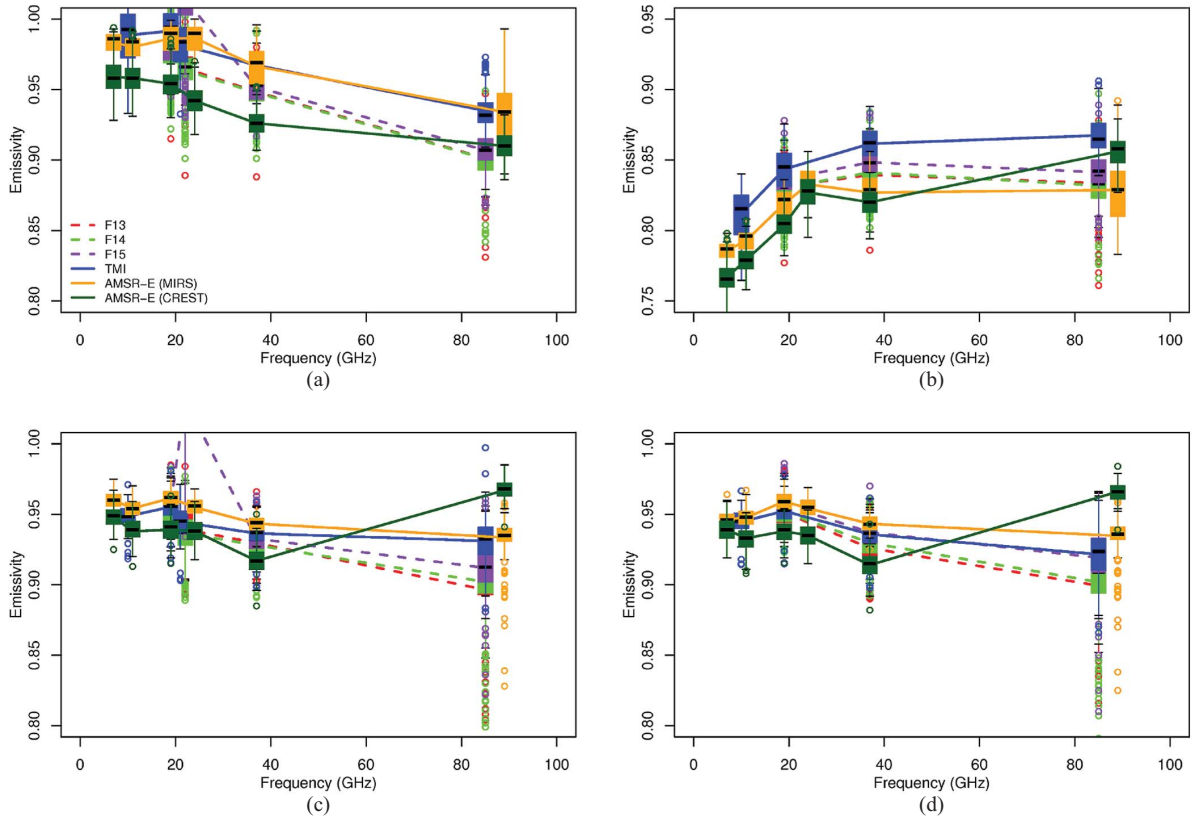

Fig. 2. Intercomparison of microwave emissivity retrievals at two LSWG sites Desert (top) and Amazon2 (bottom), over a one-year period from July 1, 2006 to June 30, 2007, for SSM/I (F13, F14, and F15), TMI and AMSR-E. Both vertical (left) and horizontal (right) polarizations are shown. The extremely high values in the vertically polarized channel of SSM/I F15 at 22.2 GHz are caused by an instrument problem documented in [33]. (a) Desert, V-pol. (b) Desert, H-pol. (c) Amazon2, V-pol. (d) Amazon2, H-pol.

(85.5/89.0 GHz) tend to have the highest spread from their mean values, suggesting again atmospheric effects are the source. The vertically polarized channel of SSM/I F15 at 22.2 GHz shows extremely high values [Fig. 2(a) and (c)]. This is caused by an instrument problem documented in [33].

Over Amazon2 [Fig. 2(a) and (d)], the magnitude of the systematic differences among the retrievals is similar to that of the Desert site, except that the differences at the higher frequencies (85.5/89.0 GHz) are much larger. Similarly, the random errors are also much higher at these frequencies. This also suggests that the atmospheric effects are playing an even larger role here, considering that Amazon2 has a much moister atmosphere and many more cloudy/rainy days than those of the desert site.

There is a lack of smoothness in the mean emissivity spectra at either site. For example, CREST's AMSR-E retrievals fashioned a bump at 23.8 GHz in its horizontal polarization at the Desert site, but it has a dip at 36.5 GHz in both polarizations at Amazon2. Other retrievals show such bumpiness in varying degrees. We believe the emissivity spectra should be smooth and monotonic, because over the frequency range being studied the land surface does not have any known physical mechanism that responds differently to a particular frequency. Thus, the roughness in the shapes of the emissivity spectra is another manifestation of systematic errors.

B. Histograms of Emissivity Retrievals

Further insight into the uncertainties can be obtained from histograms of the retrievals. Fig. 3 shows the histograms of horizontally polarized emissivities for both sites. Overall, the Desert site exhibits a gradual increase in H-pol emissivity with frequency (left) from all the retrievals, while over Amazon2 the emissivities are largely confined in the range of 0.9 to 1.0 for all the frequencies. Consistent with Fig. 2, there are considerable differences among the mean value of each of the retrievals over either site—a strong indicator of the existence of systematic errors. In addition, for each retrieval dataset, there is a range in spread around its mean emissivity value, with the shape of the histogram indicating the distribution of the random errors.

Over Amazon2, all the emissivity histograms are single mode, while over Desert, some of the retrievals, such as TMI and AMSR-E (MIRS), exhibit dual modality at some of the frequencies. We speculate this might be related to the strong diurnal cycle in the variation of the surface temperature and the microwave penetration depth, which makes it tricky to represent the effective emission characteristics in the retrieval process [9], [18], [32], [34].

C. Uncertainties in MPDI

Because MPDI can largely cancel the effect of errors in atmospheric contribution and surface temperature, we also

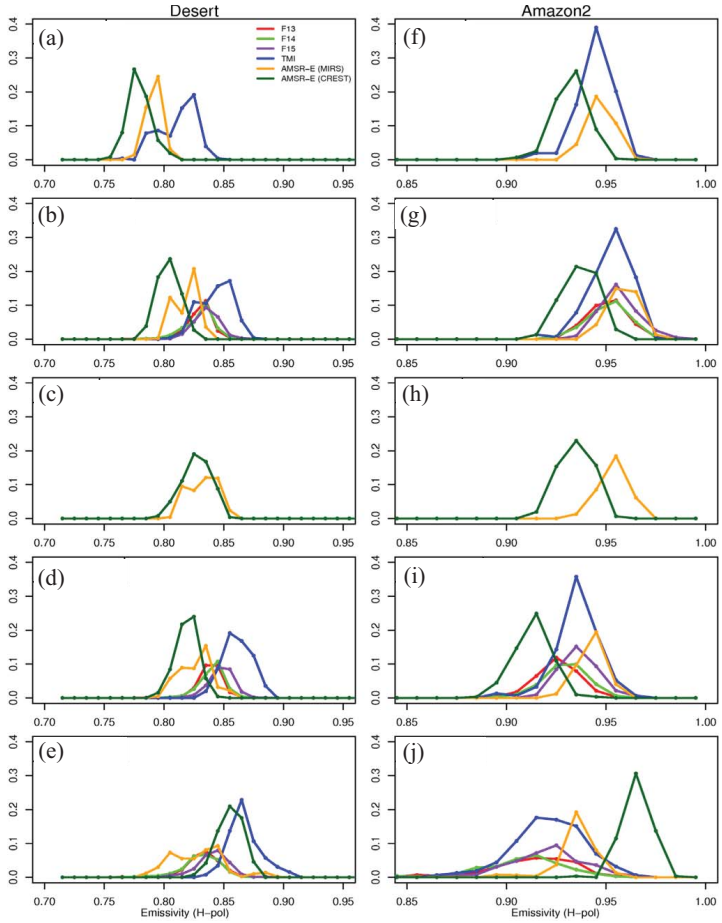

Fig. 3. Intercomparison of the histograms of the H-pol microwave emissivity retrievals at two LSWG sites Desert (left) and Amazon2 (right), over a one-year period from July 1, 2006 to June 30, 2007, for SSM/I (F13, F14, and F15), TMI, and AMSR-E, for various frequencies. (a) 10.65G. (b) 18.7/19.35G. (c) 23.8G. (d)36.5/37.0G. (e) 85.5/89.0G, (f) 10.65G. (g) 18.7/19.35G. (h) 23.8G. (i) 36.5/37.0G. (j) 85.5/89.0G.

examined the uncertainties in MPDI computed from the emissivity retrievals. This will reveal how much of the error is common in both V- and H-pol channels, and how much is not. If a significant portion of the error in an emissivity retrieval is common to both channels, MPDI will show much lower systematic and random error amplitudes than the emissivity values alone. Indeed, as shown in Fig. 4(a), MPDI values over Desert show much better agreement among the retrievals, except AMSR-E (MIRS). This suggests most of the systematic errors in the emissivity retrievals are common to both channels. In addition, the variance becomes much smaller, indicating that both channels have the same random error as well most of the times. Similar conclusions can be drawn for Amazon2 [Fig. 4(c)] for most of the frequencies, except for 85.5/89.0 GHz, which shows fairly large systematic and random errors. Obviously, the errors at the highest frequencies are larger and less co-varying between the vertical and horizontal polarizations.

For comparison, we also studied the MPDI computed from AMSR-E TOA Tb values over these two sites [Fig. 4(b) and (d)]. Interestingly, the spectral shapes between emissivity-based (Fig. 4, left) and Tb-based MPDI (Fig. 4, right) are strikingly similar. Since Tb-based MPDI is the lower bound of emissivity-based MPDI, any values in the former (Fig. 4, right) higher than those in the latter indicate systematic errors in the emissivity retrievals, such as the F15 retrievals at higher frequencies over Amazon2 [Fig. 4(c)]. In addition, there is an elbow in Tb-based MPDI at 23.8 GHz over either site, due to the strong water vapor attenuation in the atmosphere. But such a depression should not be present in emissivity-based MPDI, had the atmospheric effect been completely removed in the retrieval process. But its very existence [Fig. 4(a) and (c)] suggests otherwise. This is understandable because there is no way to recover the polarization difference from the TOA Tb if such a signal is strongly dissipated through the atmosphere. Therefore, satellite-based direct retrieval of land-surface emissivity in this frequency range (21–24 GHz) will remain a challenge, and a feasible solution is interpolation from its more transparent neighboring frequencies, as done by the tool to estimate land-surface emissivities at microwave frequencies (TELSEM) [35].

D. Error Diagnosis

To further understand the causes of the errors, we inspected the daily emissivity spectra and their variations over our 1-year period, for the various sensors for both sites. As an illustrative example, Fig. 5 shows a collage of daily emissivity retrievals from SSM/I on DMSP F13 over the Amazon2 site, for both polarizations and both morning

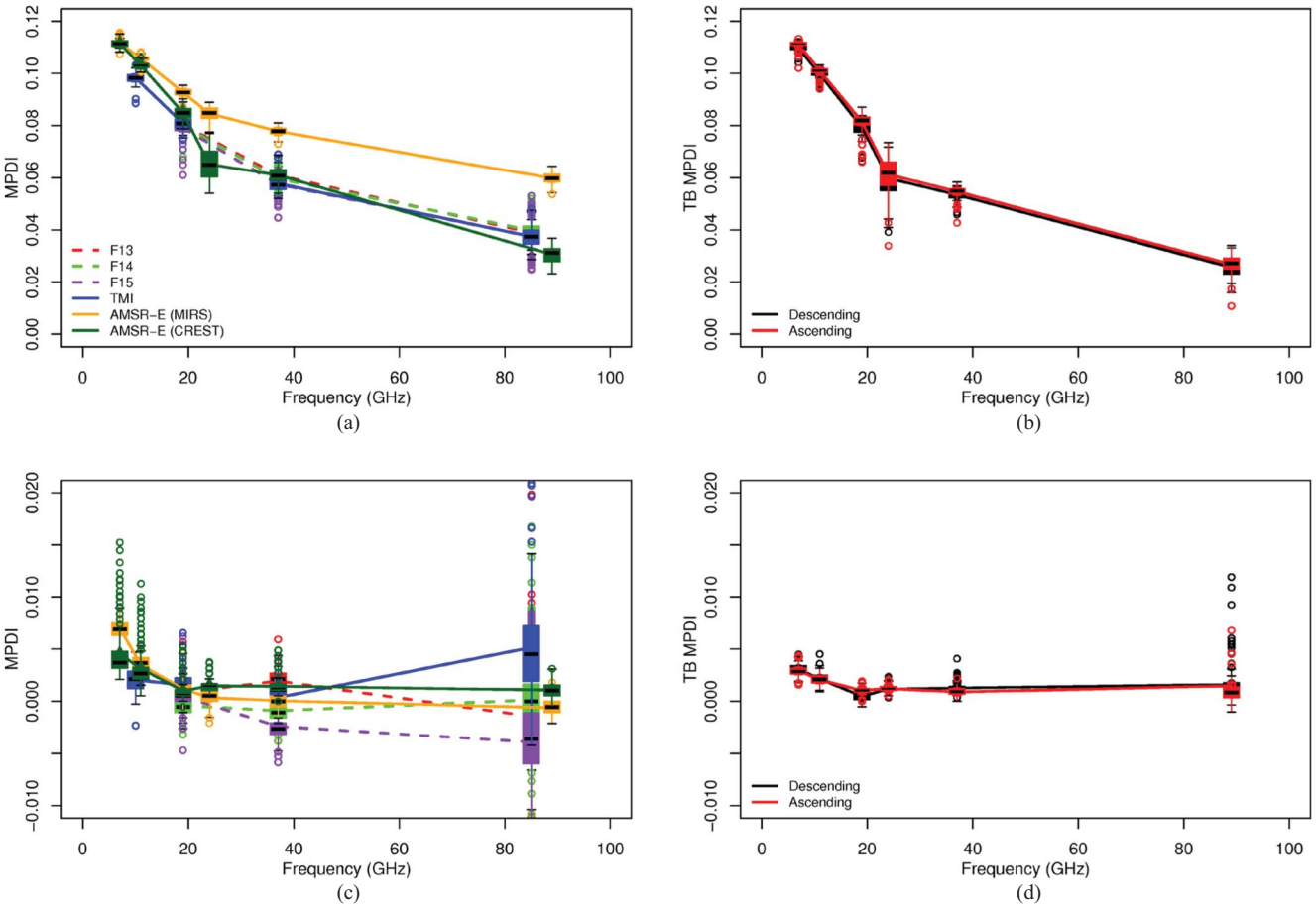

Fig. 4. Intercomparison of emissivity-based MPDI values (left) at two LSWG sites Desert (top) and Amazon2 (bottom), over a one-year period from July 1, 2006 to June 30, 2007, for SSM/I (F13, F14, and F15), TMI, and AMSR-E. For comparison, AMSR-E Tb-based MPDI values over the same two sites are also shown (right). (a) Desert, emissivity-based MPDI. (b) Desert, Tb-based MPDI. (c) Amazon2, emissivity-based MPDI. (d) Amazon2, Tb-based MPDI.

(A.M.; descending) and afternoon (P.M.; ascending) passes. The emissivities for both polarizations are of similar values, as expected over such a site. Most of the emissivity spectra are confined within the range of 0.9–1.0, but there is considerable variation, driven largely by the seasonality. This variation is more likely introduced by the errors in both land-surface temperatures and atmospheric profiles used in the retrievals. The impact of water vapor attenuation at 22.2 GHz for the vertical polarization, in the shape of an elbow, from either A.M. or P.M. passes, is obvious [Fig. 5(a) and (c)]. Such an elbow does not manifest itself in the horizontal polarization due to the lack of the 22.2 GHz [Fig. 5(b) and (d)].

Fig. 5 also reveals that the dominant source of random errors at the highest frequency (85.5 GHz) is likely the contamination from cloudy or rainy skies. As one can observe, during the morning passes, there were very few outliers at 85.5 GHz. But the afternoon passes saw a significant number of outliers with drastically reduced emissivity values in both polarizations at this frequency [Fig. 5(c) and (d)]. This coincides with the rainy time of the Amazon precipitation diurnal cycle [36], and the outliers indicate strong scattering from ice particles aloft. This suggests that the cloud screen step in the retrieval processes missed a number of cloudy and rainy conditions, resulting in enhanced random errors.

E. Analysis of Error Sources

There are numerous sources contributing to both the systematic errors and the random errors. They are identified and their relative importance is discussed as follows.

1) Differences in each of the sensors' configurations and characteristics. These include differences in the frequency, incidence angle, footprint size, overpass time, and errors in brightness temperature measurements. However, over land surfaces, the slight differences in frequencies and incidence angles among the imagers will not cause appreciable discrepancies in the retrieved emissivities, due to their weak dependencies on these two variables [23]. Also under our assumption that the radiometric properties over either the Desert or the Amazon site are sufficiently uniform and constant, the differences in footprint size and overpass time should not be considerable. The very small differences among the MPDI values (except MIRS; Fig. 4) support this assumption. In fact, even over many other types of surfaces, the emissivities from these different platforms, when retrieved with the same method and same ancillary datasets, are very close [37]. In addition, many existing calibration/validation (Cal/Val) studies [19]–[27] suggest

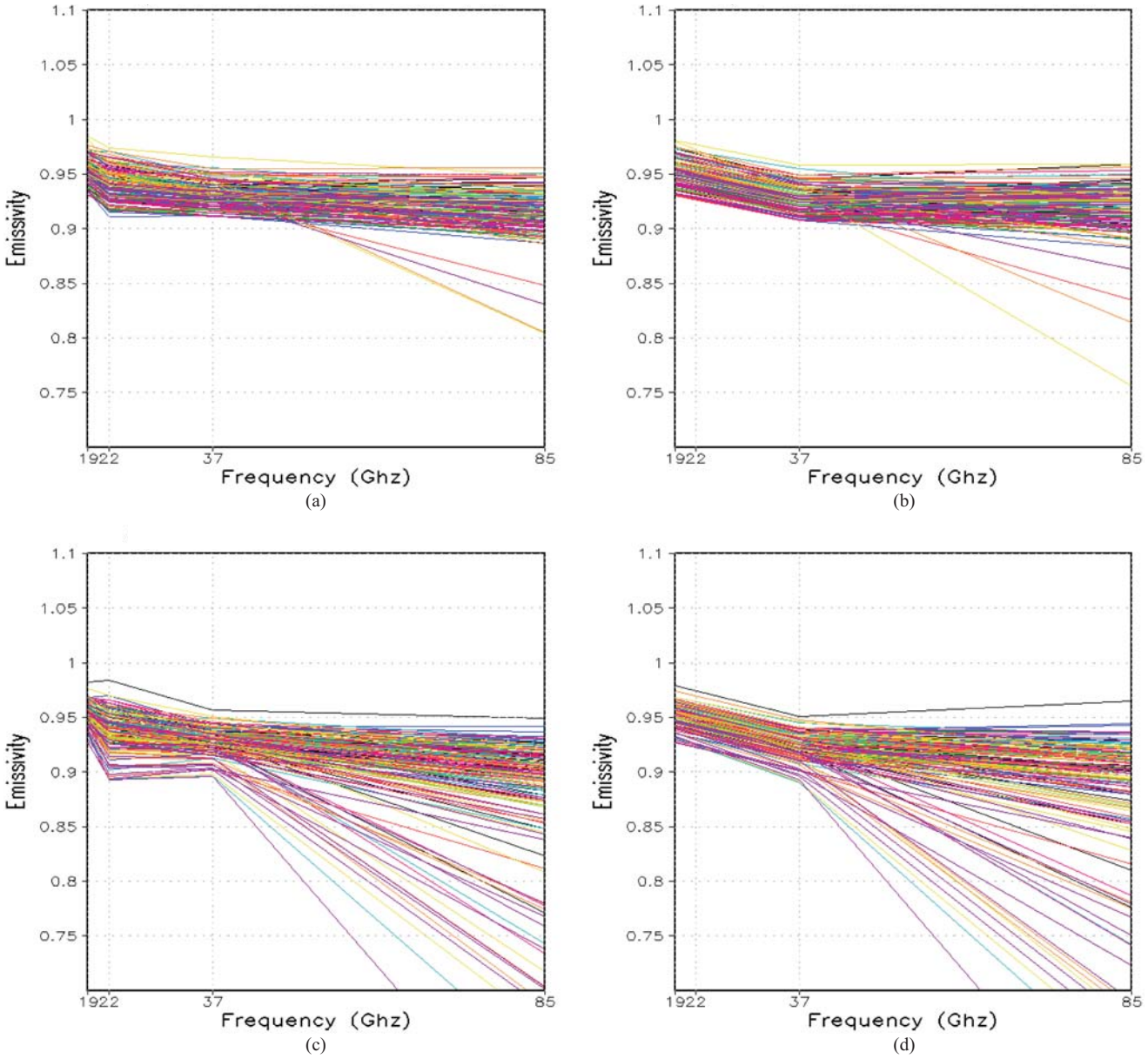

Fig. 5. Daily microwave emissivity retrievals over Amazon2 (bottom), over a one-year period from July 1, 2006 to June 30, 2007, for SSM/I F13. Both vertical (left) and horizontal (right) polarizations, as well as descending (A.M., top) and ascending (P.M., bottom) passes, are shown. Each daily retrieval is designated by a colored line. (a)–(d) Frequency (GHz).

that the systematic differences between these sensors' brightness temperature measurements are in the order of 1–3 K, much less than the error amplitude shown here. Therefore, we can infer that these factors do not dominate the errors revealed in our analysis.

2) Differences in retrieval methods. Two classes of methods are used in the retrievals: one is the variational method employed by MIRS, and the other is the direct solution of (1) and (2), used by the rest of the datasets. However, the retrieved variables from MIRS, including emissivity, will automatically satisfy (1) and (2). Therefore, if all the ancillary data are the same, theoretically both classes should produce identical results. A meaningful future effort would be testing these different retrieval methods with the same ancillary data, to verify this conclusion.

3) Differences and errors in ancillary data. Used to solve (1) and (2) for clear skies, these data include: rain/cloud masks, surface temperatures, and atmospheric temperature, and water vapor profiles. Yang and Weng [15] studied the sensitivities of emissivities retrievals to these factors with specified errors, assuming clear skies. Our results indicate that cloud/precipitation contamination plays a significant role in practice (Fig. 5), even with best-effort rain/cloud screening. In addition, the considerable systematic differences seen here, even at lower frequencies, suggest that the discrepancies in the respective ancillary datasets are even larger than [15] tested, albeit in the current it is impossible to cleanly separate the contributions from these ancillary variables. Over the Desert, the impact of the error in

TABLE II
MEAN AND STANDARD DEVIATION OF EMISSIVITY RETRIEVALS

Frequency (GHz)	6.9	10.65	18.7/19.35	21.3/22.2/23.8	36.5/37.0	85.5/89.0
Desert, V-pol						
SSM/I F13			0.976 (3.1)	0.965 (3.4)	0.948 (2.9)	0.901 (3.9)
SSM/I F14			0.975 (4.0)	0.964 (4.4)	0.948 (3.3)	0.901 (4.3)
SSM/I F15			0.980 (3.5)	~~1.014~~ (8.0)	0.952 (3.3)	0.907 (3.4)
TMI		0.989 (5.5)	0.992 (4.4)	0.982 (4.5)	0.967 (3.4)	0.935 (3.8)
AMSR-E (MIRS)	0.983 (1.9)	0.980 (2.2)	0.986 (2.7)	0.987 (2.8)	0.966 (4.0)	0.934 (6.5)
AMSR-E (CREST)	0.959 (3.7)	0.958 (3.4)	0.954 (3.0)	0.943 (3.0)	0.926 (2.6)	0.910 (2.6)
Max - Min	**0.024 (7.2)**	**0.031 (9.3)**	**0.038 (11.4)**	**0.044 (13.2)**	**0.041 (12.3)**	**0.034 (10.2)**
Desert, H-pol						
SSM/I F13			0.831 (2.8)		0.839 (2.7)	0.834 (4.3)
SSM/I F14			0.831 (3.6)		0.841 (3.1)	0.832 (4.6)
SSM/I F15			0.836 (3.1)		0.848 (2.9)	0.841 (4.0)
TMI		0.812 (4.7)	0.843 (4.1)		0.861 (3.5)	0.867 (4.0)
AMSR-E (MIRS)	0.786 (1.8)	0.793 (2.0)	0.819 (2.9)	0.833 (3.5)	0.827 (4.0)	0.829 (6.7)
AMSR-E (CREST)	0.767 (3.1)	0.779 (2.8)	0.805 (2.8)	0.827 (3.6)	0.820 (2.8)	0.856 (3.2)
Max - Min	**0.019 (5.7)**	**0.033 (9.9)**	**0.038 (11.4)**	**0.006 (1.8)**	**0.041 (12.3)**	**0.038 (11.4)**
Amazon2, V-pol						
SSM/I F13			0.953 (3.1)	0.939 (4.5)	0.930 (4.2)	0.896 (15.7)
SSM/I F14			0.951 (3.2)	0.937 (4.6)	0.928 (3.2)	0.902 (10.8)
SSM/I F15			0.958 (2.7)	~~1.030~~ (12.0)	0.933 (2.7)	0.912 (6.3)
TMI		0.949 (2.7)	0.955 (3.2)	0.945 (3.6)	0.936 (3.2)	0.931 (5.3)
AMSR-E (MIRS)	0.960 (1.5)	0.954 (1.7)	0.961 (1.9)	0.955 (1.9)	0.943 (1.8)	0.934 (4.0)
AMSR-E (CREST)	0.948 (2.3)	0.939 (2.4)	0.940 (2.6)	0.938 (2.5)	0.916 (2.9)	0.968 (1.9)
Max - Min	**0.012 (3.6)**	**0.015 (4.5)**	**0.021 (6.3)**	**0.018 (5.4)**	**0.027 (8.1)**	**0.072 (21.6)**
Amazon2, H-pol						
SSM/I F13			0.951 (3.0)		0.926 (3.2)	0.899 (16.8)
SSM/I F14			0.952 (3.1)		0.930 (3.2)	0.902 (11.5)
SSM/I F15			0.957 (2.8)		0.937 (2.8)	0.919 (6.9)
TMI		0.945 (2.7)	0.952 (3.2)		0.936 (3.2)	0.922 (5.3)
AMSR-E (MIRS)	0.947 (1.5)	0.948 (1.8)	0.959 (2.0)	0.954 (2.1)	0.943 (1.9)	0.935 (4.2)
AMSR-E (CREST)	0.939 (2.2)	0.933 (2.4)	0.938 (2.5)	0.935 (2.4)	0.914 (2.8)	0.966 (1.9)
Max - Min	**0.008 (2.4)**	**0.015 (4.5)**	**0.021 (6.3)**	**0.019 (5.7)**	**0.029 (8.7)**	**0.067 (20.1)**

Standard deviations are shown in brackets in numbers equivalent to brightness temperatures (degrees Kelvin – K), assuming a physical temperature of 300K. The range (Max-Min) of mean emissivities for each frequency also has an equivalent Tb shown in brackets.

atmospheric profile data seems insignificant, probably due to the low water vapor content in the atmosphere. Similar MPDIs (except MIRS) [Fig. 4(a)] but differing emissivities [Fig. 2(a) and (b)] suggest that the surface temperature differences and errors are primarily responsible for the systematic differences. To compound the problem, the strong diurnal variation of the surface temperature and penetration depth over desert makes it difficult to represent the effective values. On the other hand, over Amazon2, the fact that the emissivities [Fig. 2(c) and (d)] are notably different between the datasets, and the random errors in the emissivity-based MPDI [Fig. 4(c)] are much higher than those of the Tb-based MPDI [Fig. 4(d)], indicates errors in both atmospheric profile data and surface temperature data are responsible.

4) Retrievals within the water vapor attenuation band (21–24 GHz) are systematic outliers and are less reliable [e.g., Fig. 4(a) and (c)]. This is understandable because the signals from the land surface are strongly dissipated by the atmosphere, and TOA Tb measurements contain little information content originated from the land surface. Thus, direct satellite-based retrievals in this frequency range will remain a challenge. Interpolation between more transparent neighboring frequencies has been shown to be a feasible solution [35].

5) Random errors with each retrieval dataset are both frequency- and location-dependent: higher frequencies saw much more deviation from the mean values than lower frequencies (Fig. 2), and Amazon2 had more dispersion than Desert (Figs. 2 and 4). Further investigation revealed strong evidence that scattering by atmospheric hydrometeors is the dominant cause (Fig. 5), indicating the rain/cloud contamination in the presumed clear-sky retrievals. Additionally, since it consistently decreases the emissivity, the scattering process also causes a systematic drop in the mean emissivity values [e.g., Fig. 2(c) and (d)].

V. Conclusion

Due to the lack of ground-truth data, quantifying the uncertainties in satellite-based land-surface emissivity retrievals has been a challenge. We initiated an effort to evaluate such retrievals from microwave imagers over two types of land surfaces, the Sahara Desert and the Amazon Rainforest. The true emissivity over either type of land surface can be treated as virtually constant, as supported by a three-year AMSR-E Tb polarization difference record (Fig. 1). This enables us to identify both the random errors and many aspects of the systematic errors. Among the several retrieval datasets based on SSM/I, TMI, and AMSR-E that we examined, there are substantial systematic differences, especially at higher frequencies (Fig. 2). The range of the systematic differences is approximately 1%–4% of the mean values (equivalent of 3 to 12 K Tb) over the desert site and 1–7% (3 to 20 K) over Amazon, generally increasing with frequency (Table II). Within each particular dataset, the random errors are in the range of 0.5–2% (2–6 K) over both sites, except for SSM/I aboard F13 and F14, which had much larger random errors (10–17 K) over Amazon at 85.5/89.0 GHz, due to the atmospheric contamination as shown in Fig. 5.

Apparently, the retrieval of the land-surface emissivity, especially the instantaneous values, is a challenging task. In addition to factors highlighted in this paper, many other ones, such as instrument errors [33], calibration errors, differences in locations and resolutions of the satellite footprints, spatial and temporal sampling errors, and representativeness of surface properties over highly heterogeneous and dynamic surfaces (e.g., desert) [9], [18], [34], all contribute to the complexity of the retrieval process and the associated errors. It is therefore necessary to recognize the limitations in these instantaneous retrievals, and to develop strategies to alleviate their impact while extracting as much useful information as possible. For example, the monthly emissivity atlas produced by Prigent *et al.* [8] and the climatology dataset used by TELSEM [35] employ extensive quality control and long-term averaging over multiple measurements from multiple sensors. We believe these measures can dramatically reduce both the systematic and random errors.

Our paper is confined to only two sites, and the results are certainly not representative of the other types of land surfaces, or even the rainforest and desert themselves. Over highly variable surfaces, such as desert, the interplay of the error sources can differ dramatically from one site to the next. Nevertheless, we believe that the two sites over these extreme types of land surfaces give one an educated estimate on the range of errors over the land surface as a whole. This supplements another study by Ferraro *et al.* [16] which compared the systematic differences over a few LSWG sites in the continental United States. Together both studies yield considerable insights into the factors and processes affecting the uncertainties in these retrievals. Such insights will be helpful in future studies of a broader scope.

Acknowledgment

The authors would like to thank R. Ferraro and F. J. Turk for organizing the LSWG studies and C. Hernandez-Aldarondo for managing the data collection and web access. Helpful discussions with L. Li, N.-Y. Wang, X. Lin, C. Hernandez-Aldarondo, F. Weng, M. Sapiano, and other LSWG members are appreciated. The authors also would like to thank B. Choudhury, M. Kurum, E. Kim, A. Joseph, and P. O'Neil at NASA/GSFC for their consultations, and to two anonymous reviewers for their helpful comments.

References

[1] F. T. Ulaby, R. K. Moore, and A. K. Fung, *Microwave Remote Sensing: Active and Passive-Volume III: From Theory to Applications*. vol. 3, Artech House: Norwood, MA, USA, Jan. 1986.

[2] G. Skofronick-Jackson and B. T. Johnson, "Surface and atmospheric contributions to passive microwave brightness temperatures for falling snow events," *J. Geophys. Res.—Atmos.*, vol. 116, no. D2, pp. 2637–2640, Jan. 2011.

[3] Y. Tian and C. D. Peters-Lidard, "Systematic anomalies over inland water bodies in satellite-based precipitation estimates," *Geophys. Rev. Lett.*, vol. 34. no. 14, pp. 1–15, Jul. 2007.

[4] J. C. Comiso, "Sea ice effective microwave emissivities from satellite passive microwave and infrared observations," *J. Geophys. Res.*, vol. 88, no. C12, pp. 7686–7704, 1983.

[5] B. J. Choudhury, "Reflectivities of selected land surface types at 19 and 37 GHz from SSM/I observations," *Remote Sens. Environ.*, vol. 46, no. 1, pp. 1–17, Oct. 1993.

[6] C. Prigent, W. B. Rossow, and E. Matthews, "Microwave land surface emissivities estimated from SSM/I observations," *J. Geophys. Res. Atmosph.*, vol. 102, no. D18, pp. 21867–21890, Jan. 1997.

[7] A. S. Jones and T. H. V. Haar, "Retrieval of microwave surface emittance over land using coincident microwave and infrared satellite measurements," *J. Geophys. Res. Atmosph.*, vol. 102, no. D12, pp. 13609–13626, Jan. 1997.

[8] C. Prigent, F. Aires, and W. B. Rossow, "Land surface microwave emissivities over the globe for a decade," *Bull. Amer. Meteorol. Soc.*, vol. 87, no. 11, pp. 1573–1584, Nov. 2006.

[9] J. F. Galantowicz, J. L. Moncet, P. Liang, A. E. Lipton, G. Uymin, C. Prigent, and C. Grassotti, "Subsurface emission effects in AMSR-E measurements: Implications for land surface microwave emissivity retrieval," *J. Geophys. Res. Atmosph.*, vol. 116, no. D17, pp. 1–10, Sep. 2011.

[10] S. A. Boukabara, K. Garrett, C. Wanchun, F. I. Sanchez, C. Grassotti, C. Kongoli, C. Ruiyue, L. Quanhua, Y. Banghua W. Fuzhong, R. Ferraro, T. J. Kleespies, and M. Huan, "MiRS: An all-weather 1DVAR satellite data assimilation and retrieval system," *IEEE Trans. Geosci. Remote Sens.*, vol. 49, no. 9, pp. 3249–3272, Sep. 2011.

[11] M. Owe, R. de Jeu, and T. Holmes, "Multisensor historical climatology of satellite-derived global land surface moisture," *J. Geophys. Res.*, vol. 113, no. F1, pp. 1–17, Mar. 2008.

[12] T. Mo, B. J. Choudhury, T. J. Schmugge, J. R. Wang, and T. J. Jackson, "A model for microwave emission from vegetation-covered fields," *J. Geophys. Res.*, vol. 87, no. C13, pp. 11229–11237, Dec. 1982.

[13] Y. H. Kerr and E. G. Njoku, "A semiempirical model for interpreting microwave emission from semiarid land surfaces as seen from space," *IEEE Trans. Geosci. Remote Sens.*, vol. 28, no. 3, pp. 384–393, May 1990.

[14] C. Prigent, F. Aires, W. B. Rossow, and A. Robock, "Sensitivity of satellite microwave and infrared observations to soil moisture at a global scale: Relationship of satellite observations to in situ soil moisture measurements," *J. Geophys. Res.*, vol. 110, no. D11103, pp. 1–15, Jun. 2005.

[15] H. Yang and F. Weng, "Error sources in remote sensing of microwave land surface emissivity," *IEEE Trans. Geosci. Remote Sens.*, vol. 49, no. 9, pp. 3437–3442, Sep. 2011.

[16] R. R. Ferraro, P. Lidard, D. Christa, C. Hernandez, F. J. Turk, F. Aires, P. Catherine, X. Lin, B. S. Ahmed, B. Furuzawa, A. G. Fumie, H. W. Kenneth, K. Fatima, L. Li, L. Chuntao, M. Hirohiko, M. Leslie, R. Sarah, S. Jackson, M. Gail, T. Yudong, and N. Y. Wang, "An evaluation of microwave land Surface emissivities over the continental United States to benefit GPM-era precipitation algorithms," *IEEE Trans. Geosci. Remote Sens.*, vol. 51, no. 1, pp. 378–398, Jan. 2013.

[17] H. Norouzi, M. Temimi, W. B. Rossow, C. Pearl, M. Azarderakhsh, and R. Khanbilvardi, "The sensitivity of land emissivity estimates from AMSR-E at C and X bands to surface properties," *Hydrol. Earth Syst. Sci.*, vol. 15, no. 11, pp. 3577–3589, 2011.

[18] H. Norouzi, W. Rossow, M. Temimi, C. Prigent, M. Azarderakhsh, S. Boukabara, and R. Khanbilvardi, "Using microwave brightness temperature diurnal cycle to improve emissivity retrievals over land," *Remote Sens. Environ.*, vol. 123, pp. 470–482, Aug. 2012.

[19] J. P. Hollinger, J. L. Peirce, and G. A. Poe, "SSM/I instrument evaluation," *IEEE Trans. Geosci. Remote Sens.*, vol. 28, no. 5, pp. 781–790, Sep. 1990.

[20] M. C. Colton and G. A. Poe, "Intersensor calibration of DMSP SSM/I's: F-8 to F-14, 1987–1997," *IEEE Trans. Geosci. Remote Sens.*, vol. 37, no. 1, pp. 418–439, Jan. 1999.

[21] E. G. Njoku and L. Li, "Retrieval of land surface parameters using passive microwave measurements at 6–18 GHz," *IEEE Trans. Geosci. Remote Sens.*, vol. 37, no. 1, pp. 79–93, Jan. 1999.

[22] C. S. Ruf, "Detection of calibration drifts in spaceborne microwave radiometers using a vicarious cold reference," *IEEE Trans. Geosci. Remote Sens.*, vol. 38, no. 1, pp. 44–52, Jan. 2000.

[23] F. J. Wentz, P. Ashcroft, and C. Gentemann, "Post-launch calibration of the TRMM microwave imager," *IEEE Trans. Geosci. Remote Sens.*, vol. 39, no. 2, pp. 415–422, Feb. 2001.

[24] E. G. Njoku, T. Chan, W. Crosson, and A. Limaye, "Evaluation of the AMSR-E data calibration over land," *Ital. J. Remote Sens.*, vol. 29, no. 4, pp. 19–37, 2004.

[25] R. Kumar, S. A. Bhowmick, K. N. Babu, R. Nigam, and A. Sarkar, "Relative calibration using natural terrestrial targets: A preparation toward Oceansat-2 scatterometer," *IEEE Trans. Geosi. Remote Sens.*, vol. 49, no. 6, pp. 2268–2273, Jun. 2011.

[26] R. A. Kroodsma, D. S. McKague, and C. S. Ruf, "Inter-calibration of microwave radiometers using the vicarious cold calibration double difference method," *IEEE J. Sel. Topics Appl. Earth Observat. Remote Sens.*, vol. 5, no. 3, pp. 1006–1013, Jun. 2012.

[27] M. R. P. Sapiano, W. K. Berg, D. S. McKague, and C. D. Kummerow, "Toward an intercalibrated fundamental climate data record of the SSM/I sensors," *IEEE Trans. Geosci. Remote Sens.*, vol. 51, no. 3, pp. 1492–1503, Mar. 2013.

[28] S. Paloscia and P. Pampaloni, "Microwave remote sensing of plant water stress," *Remote Sens. Environ.*, vol. 16, no. 3, pp. 249–255, Dec. 1984.

[29] E. G. Njoku and I. R. Patel, "Observations of the seasonal variability of soil moisture and vegetation cover over Africa using satellite microwave radiometry," in *Proc. Int. Satellite Land-Surf. Climatology Project Conf.*, vol. 248, 1986, pp. 349–353.

[30] B. J. Choudhury, C. J. Tucker, R. E. Golus, and W. W. Newcomb, "Monitoring vegetation using Nimbus-7 scanning multichannel microwave radiometer's data," *Int. J. Remote Sens.*, vol. 8, no. 3, pp. 533–538, 1987.

[31] M. Owe, R. de Jeu, and J. Walker, "A methodology for surface soil moisture and vegetation optical depth retrieval using the microwave polarization difference index," *IEEE Trans. Geosci. Remote Sens.*, vol. 39, no. 8, pp. 1643–1654, Aug. 2001.

[32] N. C. Grody and F. Weng, "Microwave emission and scattering from deserts: Theory compared with satellite measurements," *IEEE Trans. Geosci. Remote Sens.*, vol. 46, no. 2, pp. 361–375, Feb. 2008.

[33] K. A. Hilburn and F. J. Wentz, "Mitigating the impact of RADCAL beacon contamination on F15 SSM/I ocean retrievals," *Geophys. Res. Lett.*, vol. 35, no. 18, pp. 1–11, Sep. 2008.

[34] C. Prigent, W. B. Rossow, E. Matthews, and B. Marticorena, "Microwave radiometric signatures of different surface types in deserts," *J. Geophys. Res.*, vol. 104, no. D10, pp. pp. 12147–12158, May 1999.

[35] F. Aires, C. Prigent, F. Bernardo, C. Jiménez, R. Saunders, and P. Brunel, "A tool to estimate land-surface emissivities at microwave frequencies (TELSEM) for use in numerical weather prediction," *Quart. J. Royal Meteorol. Soc.*, vol. 137, no. 656, pp. 690–699, Apr. 2011.

[36] A. J. Negri, L. Xu, and R. F. Adler, "A TRMM-calibrated infrared rainfall algorithm applied over Brazil," *J. Geophys. Res. Atmosph.*, vol. 107, no. D20, pp. LBA 15-1–LBA 15-15, Oct. 2002.

[37] F. Karbou, P. Bauer, A. Geer, and W. Bell, "Exploitation of microwave sounder/imager data over land surfaces in the presence of clouds and precipitation," EUMETSAT, Darmstadt, Germany, Tech. Rep. 37, 2008.

Yudong Tian received the Ph.D. degree in atmospheric sciences from University of California Los Angeles (UCLA), Los Angeles, CA, USA, in 1999.

He conducted research in climate dynamics and geophysical fluid dynamics at UCLA. He was one of the developers at UCLA for the popular advanced spectral analysis SSA-MTM toolkit. In 2000 and 2002, he had been working in the Internet industry, holding such positions as a Systems Manager and a Chief Technology Officer. He started to work for NASA Goddard Space Flight Center in 2002, first on the development of the Land Information System. He has been evaluating and validating satellite-based precipitation measurements, and working on land surface emissivity modeling to support NASA's Global Precipitation Measurement Mission.

Dr. Tian received the NASA's Software of the Year Award in 2005.

Christa D. Peters-Lidard received the B.S. degree (summa cum laude) in geophysics and in mathematics from the Virginia Polytechnic Institute and State University (Virginia Tech), Blacksburg, VA, USA, in 1991, and the M.A. and Ph.D. degrees from the Department of Civil Engineering and Operations Research, Water Resources Program, Princeton University, Princeton, NJ, USA, in 1993 and 1997, respectively.

She has served as the Chief of the Hydrological Sciences Laboratory at NASA's Goddard Space Flight Center, where she has been a Physical Scientist since 2001. She was an Assistant Professor with the School of Civil and Environmental Engineering, Georgia Institute of Technology, Atlanta, GA, USA, from 1997 to 2001. She is currently the Chief Editor for the American Meteorological Society (AMS) Journal of Hydrometeorology, and an elected member of the AMS Council.

Dr. Peters-Lidard has served as an Associate Editor for the Journal of Hydrology and Water Resources Research. Her current research interests include land-atmosphere interactions, soil moisture measurement and modeling, and the application of high performance computing and communications technologies in Earth system modeling, for which her Land Information System Team was awarded the 2005 NASA Software of the Year Award. She is a member of Phi Beta Kappa, and received the Committee on Space Research Scientific Commission A. Zeldovich Medal in 2004 and the Arthur S. Flemming Award in 2007. She was elected as an AMS Fellow in 2012.

Kenneth W. Harrison received the B.S. and M.S. degrees from the University of Illinois at Urbana-Champaign, Urbana, IL, USA, in 1990 and 1991, and the Ph.D. degree in civil engineering from North Carolina State University, Raleigh, NC, USA, in 2002.

He conducted research in environmental and water resources systems analysis. Applications extend from the adaptive management of water quality, water distribution systems modeling, water quantity management, assessment of the external damages of power generation, integrated solid waste management, and energy modeling. He helped to develop extensions in the NASA Land Information System to carry out uncertainty estimation via Markov chain Monte Carlo methods for Bayesian analysis for application to land surface and land surface-coupled models including microwave emissivity models. His current research interests include decision-making under uncertainty, accounting of uncertainty in modeling via Bayesian methods, the development of computationally-based decision support tools, and the optimization of large-scale systems.

Catherine Prigent received the Ph.D. degree in physics from Paris University, Paris, France, in 1988.

She has been a Researcher with the Laboratoire d'Etudes du Rayonnement et de la Matière en Astrophysique, Paris Observatory, Centre National de la Recherche Scientifique (CNRS), Paris, since 1990. From 1995 to 2000, she was on leave from CNRS and with the NASA Goddard Institute for Space Studies, Columbia University, New York, NY, USA. Her early work focused on the modeling of the sea surface emissivities at microwave wavelengths and the estimation of atmospheric parameters over the ocean from microwave measurements. She is involved in satellite remote sensing of clouds with the analysis of passive-microwave observations over convective cloud structures. Her research interests focus on passive microwave remote sensing of the Earth. Her current research interests include the calculation and analysis of microwave land surface emissivities, estimation of atmospheric and surface parameters over land from microwave observations, as well as multisatellite characterization of the land surface.

Hamidreza Norouzi received the Ph.D. degree in civil engineering (water resources) from the City University of New York (CUNY), New York, NY, USA, NOAA Cooperative Remote Sensing Science and Technology Center, based at the City College of New York in 2011.

He is currently an Assistant Professor position with the New York City College of Technology, CUNY. He has been able to retrieve land surface emissivity for more than six years from AMSR-E observations on board Aqua satellite. He is a Registered Professional Engineer. His research focus is land remote sensing using microwave measurements with focus on soil moisture and land surface emissivity. His current research interests include using satellite information in vegetation structure profile, soil moisture estimation, snow cover prediction, precipitation, and estimation of soil freeze and thaw state.

Filipe Aires received the Ph.D. degree in statistics from the University Paris–Dauphine, Paris, France, in 1999.

He was with the NASA Goddard Institute for Space Studies, New York, NY, USA, for five years as a Post-Doctoral and a Research Scientist. He obtained a Centre National de la Recherche Scientifique as a Research Scientist position with the Laboratoire de Météorologie Dynamique, Paris.

His current research interests include satellite remote sensing of the Earth and statistical analysis of the climate. He analyzed climatic signals, such as El Nino, using statistical techniques such as independent component analysis. He has defined new tools for the characterization of climate feedback. He has developed multiinstrument and multiparameter remote sensing algorithms to retrieve atmospheric variables, such as temperature, ozone, or water vapor profiles, and surface variables, such as surface skin temperature, vegetation indices, or infrared or microwave emissivities. He specialized in the exploitation of the multiwavelength synergy. Instruments involved in his work include for example IASI, AMSR-E, AMSU, HSB, MHS, SSM/I, ERS, TOVS, GOME II. He has recently developed for CNES, the French spatial agency, the SAPHIR/MADRAS water vapour algorithms for the French–Indian mission Megha-Tropiques launched in 2011. He is currently involved in various studies linked to the retrieval of IR and MW surface emissivities and atmospheric retrievals over land, such as Global Precipitation Mission. He is developing a long-term global soil moisture dataset based on multiwavelength satellite observations. He is the co-founder and CEO of Estellus, a startup in the domain of remote sensing and climate impacts.

Sid-Ahmed Boukabara received the Engineer and Master of Science degrees in signal processing from the National School of Civil Aviation, Toulouse, France, the Institut National Polytechnique de Toulouse, Toulouse, in 1994, and the Ph.D. degree in remote sensing from the Denis Diderot University, Paris, France, in 1997.

He was involved in the calibration/validation of the European Space Agency's ERS-2 microwave radiometer and has worked on the synergistic use of active and passive microwave measurements. He then joined AER Inc., Cambridge, MA, USA, as a Staff Scientist and worked on the design, implementation and validation of the NPOESS/CMIS physical retrieval algorithm, on the NASA SeaWinds/QuikSCAT wind vector rain flag and on the development of the atmospheric absorption model MonoRTM, dedicated to the microwave and laser applications. In 2005, he joined NOAA/NESDIS in Camp Springs, MD, USA, and is leading an effort to develop the capability of assimilating passive microwave measurements in all-weather conditions using a combination of variational technique algorithm and the community radiative transfer model. Since 2009, he serves as the Deputy Director of the U.S. Joint Center for Satellite Data Assimilation. His current research interests include radiative transfer modeling, spectroscopy, algorithm development, and satellite data assimilation.

Fumie A. Furuzawa received the Ph.D. degree in astrophysics from Nagoya University, Nagoya, Japan, in 2000.

She has been studying land rainfall observed with Tropical Rainfall Measuring Mission, Hydrospheric Atmospheric Research Center, Nagoya University, since 2002. She is currently working on the development of a land surface microwave emissivity algorithm with satellite measurements in order to improve rain retrieval for the development of DPR/GMI combined algorithm as part of Japan Aerospace Exploration Agency Global Precipitation Measurement mission projects.

Hirohiko Masunaga received the Ph.D. degree in astrophysics from the University of Tokyo, Tokyo, Japan, in 1999.

He has since been engaged primarily in satellite data analyses with focus on tropical meteorology and climatology including convectively-coupled equatorial waves and moist convective dynamics. He is involved in the Global Precipitation Measurement as a PI of Japan Aerospace Exploration Agency Precipitation Measuring Mission. He is currently an Associate Professor with Nagoya University, Nagoya, Japan.